Impact of 3-D Clouds on Clear-Sky Reflectance and Aerosol Retrieval in a Biomass Burning Region of Brazil

Guoyong Wen, Alexander Marshak, and Robert F. Cahalan

***Abstract*—Three-dimensional (3-D) cloud radiative effects on clear-sky reflectances and associated aerosol optical depth retrievals are quantified for a cumulus cloud field in a biomass burning region in Brazil through a Monte Carlo simulation. In this study the 1-km Moderate Resolution Imaging Spectroradiometer cloud optical depth and surface reflectance datasets are used to compute the 3-D radiation fields with ambient aerosol optical thickness of 0.1 at a wavelength of 0.66 μm. The 3-D radiative effects range from -0.015 to 0.018 with an average of 0.004 and standard deviation of 0.006. The 3-D effects are most pronounced and variable for cloud neighboring pixels, where both large negative effects over shadows and positive effects near sunlit cloud edges are found. The clear next-to-cloud pixels, that contain $\sim$83% of the clear pixel population, are affected in the most complex way and not reliable for aerosol retrieval. In the area 2 km away from clouds, the 3-D effects enhance the reflectance in clear patches. The average and variability of enhancements gradually decrease as a function of the cloud-free distance, resulting in a systematically higher aerosol optical depth estimates for pixels closer to clouds in one-dimensional (1-D) retrieval. At a distance of 3 km away from clouds, the 3-D effect is still appreciable with the average enhancement slightly less than 0.004. This enhancement will lead to an over estimate of aerosol optical thickness of $\sim$0.04 in 1-D retrieval, which is significant for an ambient atmosphere with aerosol optical thickness of 0.1.**

***Index Terms*—Aerosols, clouds, International Intercomparison of 3D Radiation Codes (I3RC), scattering, solar radiation, three-dimensional (3-D) radiative transfer.**

I. Introduction

SINCE Twomey [17] proposed the theory on the effect of aerosol on cloud properties, much research has been conducted to understand how aerosols modify clouds (e.g., [4]–[6], [9]). Although more satellite data have become available to allow scientists to investigate aerosol–cloud interaction on a global scale, to quantify this interaction through satellite observations still remains a great challenge. To achieve this goal one needs to accurately determine both the ambient aerosol amounts and associated cloud properties. However, the large contrast between optically thin aerosols and optically thick clouds intramixed with each other makes it difficult to determine the aerosol amount with one-dimensional (1-D) retrievals because, in general, this is an essentially three-dimensional (3-D) problem.

In the past few years, efforts have been made to quantify 3-D radiative effects of clouds on the aerosol retrieval in nearby cloud-free region. For example, 3-D radiative effects of clouds on reflected sunlight have been observed from Landsat images [2], [19], and a parameterization method was proposed to quantify such effects [19]. Extensive 3-D Monte Carlo simulations were performed for cuboidal bar- and cubic-shaped clouds to estimate the effects of clouds on surface reflectance and aerosol retrievals from satellite observations [2].

This letter is an extension of our previous research. In contrast to earlier 3-D modeling studies, this work is based on a realistic cumulus cloud field in a biomass burning region in Brazil. State-of-the-art 3-D Monte Carlo (MC) radiative transfer models [3], [12] make it possible to accurately compute the radiation fields in complex cloudy atmospheric conditions. In this letter, optical properties of cloud field, aerosols, and surfaces for the 3-D computation are described in Section II. Section III provides the results of the study followed by a summary and discussion of the results in the final section.

II. Cloud, Aerosol, and Surface Properties

Fig. 1 shows a 1-km resolution cloud optical depth image retrieved from Moderate Resolution Imaging Spectroradiometer (MODIS) observations [15]. The image is centered on the equator at 53.78° west and was taken on January 25, 2003 with solar zenith angle of 32° and solar azimuth angle of 129° and nadir viewing geometry. The domain of the simulation is 80 $\times$ 68 at 1-km resolution, which completely covers an Advanced Spaceborne Thermal Emission and Reflection Radiometer (ASTER) image of size $\sim$ 60 km $\times$ 60 km [18]. The cloud cover is 53%. The phase function at 0.66 μm is computed assuming a gamma distribution of cloud droplet with effective radius of 10 μm and effective variance of 0.1 [7]. The cloud-top height is determined from the brightness temperature at 11 μm from MODIS channel 31, and the cloud base is assumed constant at 1 km. We also assume a linear vertical profile of cloud liquid water. The case is chosen for the increasing interest in cloud aerosol interaction research in the biomass burning region (e.g., [1]) and was selected as a phase 3 case for the

Manuscript received May 13, 2005; revised August 23, 2005. This work was supported in part by the National Aeronautics and Space Administration's Radiation Program and EOS Program under Grants 622-42-57-20 and 621-30-86-20 and in part by the Department of Energy's ARM program under Grant DE-AI02-00ER62939.

G. Wen is with the NASA Goddard Space Flight Center, Greenbelt, MD 20771 USA and also with Goddard Earth Sciences and Technology Center, University of Maryland Baltimore County, Baltimore, MD 21228 USA (wen@climate.gsfc.nasa.gov).

A. Marshak and R. F. Cahalan are with the NASA Goddard Space Flight Center, Greenbelt, MD 20771 USA.

Digital Object Identifier 10.1109/LGRS.2005.861386

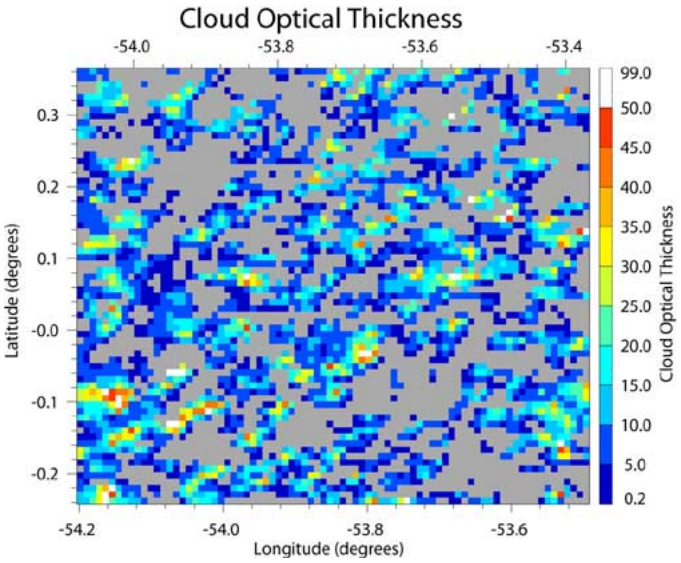

Fig. 1. Cloud optical thickness field from MODIS retrievals. Clear pixels are in gray.

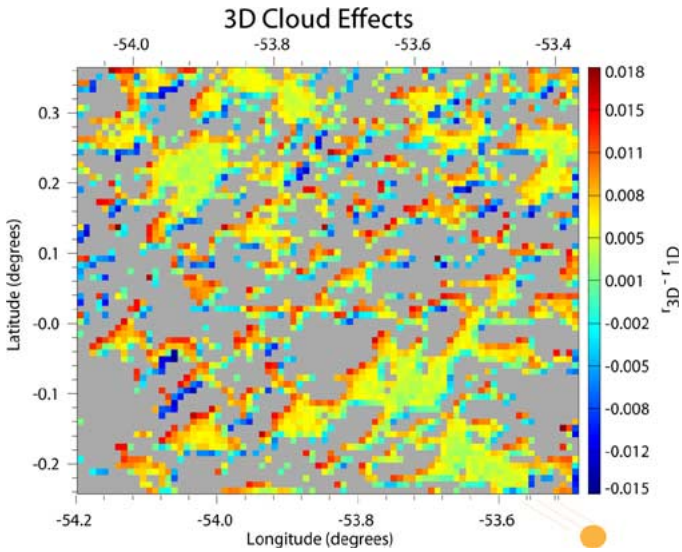

Fig. 2. Three-dimensional radiative effects of cloud on reflectance of clear pixels with the direction of incident solar radiation indicated. Cloudy pixels are in gray.

I3RC [3]. This scene is also typical for fair weather cumulus, as discussed in Section III.

The aerosol is assumed to have a lognormal size distribution with log of standard deviation of 0.7 and effective radius of 0.13 μm. The single scattering albedo is 0.93. The aerosol amount with optical thickness of 0.1 is assumed to be uniformly distributed in two layers, with the lower troposphere below 2 km and the free troposphere above. The aerosol optical thickness in the free troposphere is assumed to be 0.01 with remaining aerosols in the lower troposphere. Rayleigh scattering is also taken into account.

The value-added surface datasets derived from MODIS land products [13] show that the surface in the region is covered by vegetation: it is dark and homogeneous in the visible wavelength at 0.66 μm. The average white-sky and black-sky albedos [13] in the region are 0.025 and 0.021 with standard deviations of 0.004 and 0.003, respectively. For simplicity, a Lambertian surface with albedo of 0.023 is used as a lower boundary condition.

III. Three-Dimensional Radiative Effects

A 3-D MC scheme [3], [12] is used to compute the nadir reflectance at 0.66 μm for cloud, atmospheric optical, surface properties, and sun angle as described in Section II. Since the 3-D radiative effects of clouds on clear-region reflectances are the primary interest in this study, we compare the "true" reflectance fields from a full 3-D simulation with its 1-D counterpart only for clear pixels. The 3-D radiative effect of cloud is defined as $r_{3D} - r_{1D}$, where r_{3D} is the "true" reflectance of a clear pixel in the cumulus field calculated using a full 3-D simulation while r_{1D} is its 1-D counterpart. A small variation in viewing geometry (about $\pm 3^{\circ}$ in viewing zenith angle) is ignored in computing the nadir reflectances. For this cloud-free atmosphere, the reflectance is $r_{1D} = 0.0435$.

The 3-D cloud effects at pixel level are presented in Fig. 2. The clouds are indicated as gray. It is evident that cumulus clouds could either reduce (negative effect) or enhance (positive effect) the clear region reflectance with the 3-D effects ranging from -0.015 to 0.018. There are two important features immediately identified from Fig. 2. First, clouds cast shadows on the ground leading to large reductions of reflectance over shadowed pixels. Second, clouds enhance clear-region reflectance everywhere else. The largest enhancements are found for clear pixels adjacent to the sunlit side of clouds. The overall and detailed statistics of the enhancement are described below.

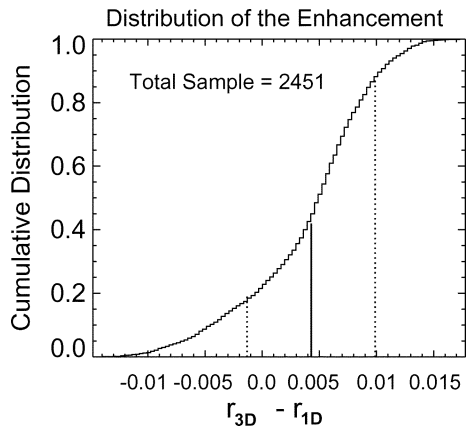

Fig. 3. Cumulative distribution of the 3-D effect with the average ($\sim$0.0043) indicated by the solid line, and one standard deviation ($\sim$0.0056) from the average indicated by the dotted lines. The cloud free 1-D reflectance is 0.0435.

Fig. 3 shows the cumulative distribution of 3-D effects for all clear pixels. The average 3-D effect is about 0.004 with standard deviation about 0.006. The distribution of the 3-D effects is asymmetric indicating different origins in the population of the distribution. The long tail of negative 3-D effects extending to -0.015 comes from shadowed pixels, while the large value of 3-D effects at the end of the positive tail comes from pixels adjacent to the sunlit side of clouds as explained in detailed analysis below.

It is interesting to examine the statistics of reflectance for pixels with the same distance away from the nearest cloud. The nearest cloud distance of a clear pixel is defined as the distance from the center of that pixel to the center of the nearest cloudy

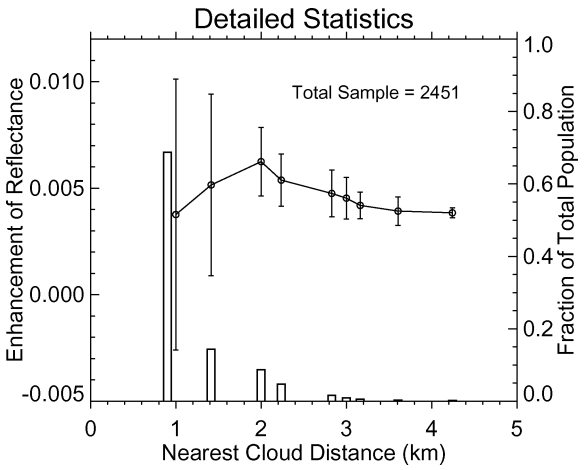

Fig. 4. Average enhancement (circles, left scale) and standard deviation (vertical brackets) for clear pixels with different nearest cloud distance. Vertical bars show the fraction of clear pixels (right scale) as a function of the nearest cloud distance. The first bar at 1 km nearest cloud distance is shifted slightly for clarity.

pixel. In a discrete grid field, the nearest cloud distance (d) is calculated from the difference in rows (Δi) and columns (Δj) between the clear and cloud pixels and the grid size ds, i.e., $d = \sqrt{\Delta i^2 + \Delta j^2} ds$. For a grid size of 1 km only a discrete set $(d_1, d_2, d_3, d_4, d_5, \ldots)$ or $(1, \sqrt{2}, \sqrt{5}, 2\sqrt{2}, 3, \ldots)$ (km) of nearest cloud distance is allowed. The nearest cloud distance not only gives a measure of the distance between a clear pixel and the nearest cloudy pixel, but also determines the range of a completely clear area from that clear pixel. For a given clear pixel with the nearest cloud distance of d_k, the area with a radius of d_{k-1} around this pixel is completely clear.

Fig. 4 shows the statistics of the enhancement for clear pixels with different nearest cloud distances. It is apparent that the reflectance statistics (circles) falls into two categories. The first one $(d < 2$ km) is classified as "cloud neighboring region," and the second one $(d \geq 2$ km) as "open area." In the cloud neighboring region, the reflectance is largely enhanced or reduced for clear pixels depending on sunlit or shadowed side of clouds. This results in a large variability in the 3-D effects. The variabilities of the 3-D effect as measured by the standard deviation are 0.006 and 0.004 for pixels next to clouds $(d = 1$ km) and pixels diagonally next to clouds $(d = \sqrt{2}$ km), respectively. Since the variability in the 3-D effect is so large, the cloud neighboring pixels are absolutely not reliable for aerosol retrieval.

The average 3-D effect in the cloud neighboring region is a result of a competition between shadowing reduction and diffuse enhancement. For a dark surface with 0.023 surface albedo, the average 3-D effect is positive. Moving away from clouds, the diffuse enhancement dominates and the average enhancement of reflectance increases, reaching a maximum about 0.006 at nearest cloud distance of 2 km, then decreases monotonically. The increase in the average of the enhancement within the cloud neighboring region is primarily due to the fact that the ratio of shadowing pixels to the total pixels decreases with the distance as shadowing diminishes and as one moves farther away from clouds, the number of negative extreme values decreases resulting in a decrease in the variability of the 3-D effect.

In the open area with $d \geq 2$ km, both the average 3-D effect and the associated variability decrease gradually as a function of nearest cloud distance, leading to a systematically higher 1-D retrieval of aerosol optical thickness for clear pixels closer to clouds. At a distance of 3 km away from clouds, the average enhancement reduces to 0.0045 with a standard deviation of 0.001. However, the enhancement does not decrease to zero within the cloud field. Rather, the enhancement reaches an appreciable value slightly less than 0.004. This enhancement will result in an overestimate of AOD of 0.04 in 1-D retrieval. The error is still significant for an atmosphere with true ambient aerosol optical thickness of 0.1.

Also, it should be noted that the cloud neighboring clear pixels contain 68.8% of the total clear pixel population of 2541 (Fig. 4). This fraction will be 83.2% if clear pixels diagonally next to a cloud are included. With strong variability in the 3-D effects, this large amount of cloud neighboring pixels appears not reliable in simple 1-D retrieval. Away from clouds, the clear pixel population drops rapidly. The clear pixel population falls to less than 2% of the total population for $d \geq 3$ km. The distribution resembles cloud spacing distributions both from satellite and ground based observations (i.e., [8, Fig. 2] and [11, Figs. 6 and 7]) and is probably typical for fair weather cumulus. Such rapid decrease in clear pixel population away from cloud in a fair weather cumulus region is an obstacle for any efforts to use clear pixels far away from clouds for retrieval of aerosol optical properties.

IV. Summary and Discussions

Three-dimensional radiative effects on clear-region reflectance and aerosol retrievals are quantified for a realistic cumulus cloud field over a dark surface with Lambertian albedo of 0.023 over a biomass burning region in Brazil. The results show that clouds cast shadows to reduce the reflected sunlight and enhance reflectance almost everywhere else in clear patches in cumulus cloud fields. The 3-D effect ranges from -0.015 to 0.018 with an average of 0.004 and standard deviation of 0.006 for all clear pixels. The relatively small average effect is primarily due to the diffusive enhancement compensated by relatively large shadowing reduction in the domain average.

Detailed analyses show that the reduction of reflectance occurs over cloud shadows. Large enhancement in reflectance is found for pixels next to the sunlit side of clouds. The average enhancement of clear-region reflectance increases as a function of the nearest cloud distance reaching a maximum at the nearest cloud distance of 2 km, and decreases monotonically. Within the cloud neighboring region, the increase in the average enhancement away from clouds is primarily due to a decrease in the ratio of shadowed pixels to the total number of pixels as a function of the distance from clouds, and a much larger shadowing reduction effect than diffuse enhancement effect. Cloud neighboring pixels, including those diagonally next to clouds, which contain $\sim$83% of all clear pixel population, are affected in a complex way, with large variability in 3-D effect. Therefore, cloud neighboring pixels are not reliable for aerosol retrieval.

In the open area, the enhancement of reflectance and associated variability decrease gradually as a function of nearest cloud

distance resulting in systematically higher 1-D aerosol optical thickness retrieval for pixels closer to clouds. As the distance to the nearest cloud increases, the clear pixel population drops rapidly adding additional difficulties in aerosol retrieval. The population of clear pixels with nearest cloud distance $d \geq 3$ km drops to less than 2% of the total clear pixel population. It should be noted that clear pixels at a distance of 3 km away from clouds are still affected by clouds with the enhancement slightly less than 0.004. This enhancement corresponds to an over-estimate of aerosol optical depth of 0.04 in 1-D retrieval which is still significant for an atmosphere with ambient aerosol optical depth of 0.1.

One should notice that 3-D effects of real fair weather cumulus are appreciably different from those of a simple shaped isolated optically thick cloud. First, the open space in a fair weather cumulus is rather limited to a range of less than 4 km. Second, at a distance 4 km away from clouds in the clear region, the fair weather cumulus imposes larger effects on clear region reflectance with enhancement of $\sim$0.004 for fair weather cumulus versus enhancement $\sim$0.002 for a single optically thick cloud (e.g., [2, Fig. 11]). The larger enhancement about 0.004 is consistent with the enhancement in path radiance at both red and blue bands observed from Landsat imagery (e.g., [19, Fig. 8]). This discrepancy is primarily due to the fact that the open area is surrounded by puffy clouds in a realistic fair weather cumulus field, which effectively produces diffuse radiation, resulting in a higher enhancement in open area reflectance.

We also found that the vertical distribution of aerosols affects the enhancement. For the same amount of aerosols, the higher the altitude of aerosols, the larger the enhancement, and the smaller the shadowing reduction in clear-region reflectance. One should notice that the aerosol is assumed horizontally uniformly distributed in this study. In the real world, aerosol properties in the vicinity of clouds may vary, making for even more complicated aerosol retrieval. The magnitude of 3-D effects also depends on solar zenith angle as discussed by Nikolaeva *et al.* [14].

Finally, we conclude that 3-D radiative effects of clouds are important in quantifying ambient aerosol amounts in a cumulus cloud field. Furthermore, special caution must be made in applying 1-D techniques or using 1-D retrieved aerosol data in aerosol-cloud interaction research.

ACKNOWLEDGMENT

The authors thank L. Remer for useful discussions.

REFERENCES

[1] M. O. Andreae, D. Rosenfeld, P. Artaxo, A. A. Costa, G. P. Frank, K. M. Longo, and M. A. F. Silva-Dias, "Smoking rain clouds over the Amazon," *Science*, vol. 303, pp. 1337–1342, Feb. 27, 2004.

[2] R. F. Cahalan, L. Oreopoulos, G. Wen, A. Marshak, S.-C. Tsay, and T. DeFelice, "Cloud characterization and clear sky correction from Landsat 7," *Remote Sens. Environ.*, vol. 78, pp. 83–98, 2001.

[3] R. F. Cahalan *et al.*, "The International Intercomparison of 3-D Radiation Codes (I3RC): Bringing together the most advanced radiative transfer tools for cloudy atmospheres," *Bull. Amer. Meteorol. Soc.*, vol. 86, no. 9, pp. 1275–1293, 2005.

[4] J. A. Coakley, Jr., R. L. Bernstein, and P. A. Durkee, "Effect of ship-track effluents on cloud reflectivity," *Science*, vol. 237, pp. 1020–1022, 1987.

[5] G. Feingold, "Modeling of the first indirect effects: analysis of measurement requirements," *Geophy. Res. Lett.*, vol. 30, no. 19, p. 1997, 2003. DOI: 10.1029/2003GL017967.

[6] Q. Han, W. Rossow, and A. Lacis, "Near-global survey of effective droplet radii in liquid water cloud using ISCCP data," *J. Clim.*, vol. 7, pp. 465–497, 1994.

[7] J. Hansen, "Multiple scattering of polarized light in planetary atmospheres. Part II. Sunlight reflected by terrestrial water clouds," *J. Atmos. Sci.*, vol. 28, pp. 1400–1426, 1971.

[8] J. H. Joseph and R. F. Cahalan, "Nearest neighbor spacing of fair weather cumulus clouds," *J. Appl. Meteorol.*, vol. 29, pp. 793–805, 1990.

[9] Y. Kaufman and R. Fraser, "The effect of smoke particles on clouds and climate forcing," *Science*, vol. 277, pp. 1636–1639, 1997.

[10] Y. Kaufman *et al.*, "A critical examination of the residual cloud contamination and diurnal sampling effects on MODIS estimates of aerosol over ocean," *IEEE Trans. Geosci. Remote Sens.*, vol. 43, no. 12, pp. 2886–2897, Dec. 2005.

[11] D. E. Lane, K. Goris, and R. C. J. Somerville, "Radiative transfer through broken clouds: Observations and model validation," *J. Clim.*, vol. 15, pp. 2921–2933, 2002.

[12] A. Marshak and A. Davis, *3-D Radiative Transfer in Cloudy Atmospheres*. Berlin, Germany: Springer-Verlag, 2005.

[13] E. G. Moody, M. D. King, S. Platnick, C. B. Schaaf, and F. Gao, "Spatially complete global spectral surface albedos: Value-added datasets derived from Terra MODIS land products," *IEEE Trans. Geosci. Remote Sens.*, vol. 43, no. 1, pp. 144–158, Jan. 2005.

[14] O. V. Nikolaeva, L. P. Bass, T. A. Germogenova, A. A. Kokhanovisky, V. S. Kuznetsov, and B. Mayer, "The influence of neighboring clouds on the clear sky reflectance with the 3-D transport code RADUGA," *J. Quant. Spectrosc. Radiat. Transf.*, vol. 94, pp. 405–424, 2005.

[15] S. Platnick, M. King, S. Ackerman, W. P. Menzel, B. Baum, J. C. Riedi, and R. A. Frey, "The MODIS cloud products: Algorithms and examples from Terra," *IEEE Trans. Geosci. Remote Sens.*, vol. 41, no. 2, pp. 459–473, Feb. 2003.

[16] L. Remer *et al.*, "The MODIS aerosol algorithm, products, and validation," *J. Atmos. Sci.*, vol. 62, pp. 947–973, 2005.

[17] S. Twomey, "The influence of pollution on the shortwave albedo of clouds," *J. Atmos. Sci.*, vol. 34, pp. 1149–1152, 1977.

[18] Y. Yamaguchi, A. B. Kahle, H. Tsu, T. Kawakami, and M. Pniel, "Overview of Advanced Spaceborne Thermal Emission and Reflection Radiometer (ASTER)," *IEEE Trans. Geosci. Remote Sens.*, vol. 36, no. 4, pp. 1062–1071, Jul. 1998.

[19] G. Wen, R. F. Cahalan, S.-C. Tsay, and L. Oreopoulos, "Impact of cumulus cloud spacing on Landsat atmospheric correction and aerosol retrieval," *J. Geophys. Res.*, vol. 106, pp. 12 129–12 138, 2001.